

# Bio-nanowebs Based on Poly(styrene- $\beta$ -isobutylene- $\beta$ -styrene) (SIBS) Containing Single-Wall Carbon Nanotubes

Yong Liu, Kerry J. Gilmore, Jun Chen,\*  
Violeta Misoska, and Gordon G. Wallace\*

ARC Centre of Excellence for Electromaterials Science  
Intelligent Polymer Research Institute, University of  
Wollongong, Wollongong NSW 2522, Australia

Received January 1, 2007

Revised Manuscript Received April 10, 2007

Electrospinning provides a simple, rapid, and inexpensive way to produce nano/microscaled polymer fibers using electrostatic force.<sup>1–4</sup> Electrospun products have been widely employed in areas such as high-performance filters,<sup>5</sup> high-surface-area electrodes,<sup>6</sup> and fiber templates.<sup>7</sup> Recently, electrospinning of nanofibrous polymer scaffolds for tissue engineering applications has attracted attention. A biodegradable poly (lactic-co-glycolic acid) (PLGA) material containing chitin was electrospun from hexafluoro propanol and formic acid solution.<sup>8</sup> Others have electrospun chitosan fibers from trifluoroacetic acid solutions<sup>9</sup> and aliphatic polyesters (such as poly( $\epsilon$ -caprolactone)) from methylene chloride and dimethyl formamide.<sup>10</sup> In the quest for biocompatible/bioresorbable, electrospinning has been used to produce nanostructured dextran membranes.<sup>11</sup>

Poly(styrene- $\beta$ -isobutylene- $\beta$ -styrene) (SIBS) is a block copolymer first reported by Kennedy<sup>12,13</sup> that exhibits different microphase morphologies depending on the ratio of styrene to isobutylene units in the copolymer. Compositions that result in SIBS structures consisting of a continuous polyisobutylene phase and discontinuous polystyrene phases provide a material that exhibits mechanical properties similar to an elastomer.<sup>14</sup> SIBS is biostable<sup>15–17</sup> and has been used

as a biocompatible drug-eluting coating for cardiac stents.<sup>18–21</sup> An increasing electronic conductivity in implantable materials has been shown to result in a decrease in the foreign body response.<sup>22</sup> It also provides the basis of electrode materials that may be used to provide electrical stimulation to control cell behavior.<sup>23</sup> Carbon nanotubes, first discovered by Iijima in 1991,<sup>24</sup> possess a fascinating combination of electronic and mechanical properties and their potential application as components of novel biomaterials has not gone unnoticed.<sup>25,26</sup> Carbon nanotube platforms have been successfully used for the growth of the mouse fibroblast line L-929<sup>27</sup> as well as neuronal cells,<sup>28,29</sup> smooth muscle cells,<sup>30</sup> and in bone-cell proliferation.<sup>31</sup>

In the present work, nanofibers of SIBS and single-wall carbon nanotubes (SWNTs) were prepared using electrospinning. The electrospun fiber webs consisted of an interconnected microporous structure. These structures have potential advantages of enhanced mass transport and provision of interpenetrating 3D networks for cell attachment and proliferation. Although our initial goal in this work was to produce conductive electroactive 3D networks based on SIBS, the addition of SWNTs was also found to facilitate the electrospinning process.

Solution conductivity, surface tension, and viscosity are key parameters in determining the suitability of polymer solutions for electrospinning.<sup>32</sup> These properties were determined for each of the SIBS/SWNT dispersions investigated

\* Corresponding author. E-mail: gwallace@uow.edu.au.

- (1) Formhals, A. U. S. Patent 1 975 504, 1934.
- (2) Shin, Y. M.; Hohman, M. M.; Brenner, M. P.; Rutledge, G. C. *Polymer* **2001**, *42*, 9955.
- (3) Fong, H.; Reneker, D. H. Electrospinning and Formation of Nanofibers. In *Structure Formation in Polymer Fibres*; Salem, D. R., Sussman, M. V., Eds.; Chapter 6; Hanser, Munich, 2001; pp 225.
- (4) Yarin, A. L.; Koombhongse, S. *J. Appl. Physics* **1990**, *9*, 4836.
- (5) Bognitzki, M.; Czado, W.; Frese, T.; Wendoff, J. H. *Adv. Mater.* **2001**, *13*, 70.
- (6) Huang, L.; Mcmillan, R. A.; Apkarian, R. P.; Pourdeyhi, B.; Chaikof, E. L. *Macromolecules* **2000**, *33*, 2989.
- (7) Bognitzki, M.; Hou, H.; Ishaque, M.; Frese, T.; Hellwig, M.; Schwarte, C.; Schaper, A.; Wendorff, J. H.; Grwiner, A. *Adv. Mater.* **2000**, *12*, 637.
- (8) Min, B. M.; You, Y.; Kim, J. M.; Lee, S. J.; Park, W. H. *Carbohydr. Polym.* **2004**, *57*, 285.
- (9) Ohkawa, K.; Cha, D.; Kim, H.; Nishida, A.; Yamamoto, H.; *Macromol. Rapid Commun.* **2004**, *25*, 1600.
- (10) Lee, K. H.; Kim, H. Y.; Khil, M. S.; Ra, Y. M.; Lee, D. R. *Polymer* **2003**, *44*, 1287.
- (11) Jiang, H.; Fang, D.; Hsiao, B. S.; Chu, B.; Chen, W. *Biomacromolecules* **2004**, *5*, 326.
- (12) Kaszas, G.; Puskas, J. E.; Hager, W. G.; Kennedy, J. P. US Patent, 4 946 899, 1990.
- (13) Kaszas, G.; Puskas, J. E.; Hager, W. G.; Kennedy, J. P.; Chen, C. C. *J. Macromol. Sci., Pure Appl. Chem.* **1989**, *25* (8), 1099.
- (14) Puskas, J. E.; Kaszas, G. *Prog. Polym. Sci.* **2000**, *25*, 404.
- (15) Pinchuk, L.; Kahn, J.; Martin, J. B.; Wilson, G. J. *Trans. World Biomater. Congr.* **2001**, 1452.
- (16) Pinchuk, L.; Nott, S.; Schwarz, M.; Kamath, K. US Patent 6 545 097, April 8, 2003.
- (17) Pinchuk, L.; Nott, S.; Schwarz, M.; Kamath, K. US Patent 20030171496, Sept 11, 2003.
- (18) Stone, G. W.; Ellis, S. G.; Cox, D. A.; Hermiller, J.; O'Shaughnessy, C.; Mann, J. T.; Turco, M.; Caputo, R.; Bergin, P.; Greenberg, J.; Popma, J. J.; Russell, M. E. for the TAXUS-IV Investigators. *N. Engl. J. Med.* **2004**, *350*, 221.
- (19) Grube, E.; Silber, S.; Hauptmann, K. E.; Mueller, R.; Buellesfeld, L.; Gerckens, U.; Russel, M. E. TAXUS I. *Circ. Clin. Invest. Rep.* **2002**, *106*, 76.
- (20) Colombo, A.; Drzewiecki, J.; Banning, A.; Grube, E.; Hauptmann, K.; Silber, S.; Dudek, D.; Fort, S.; Schiele, F.; Zmudka, K.; Guagliumi, G.; Russell, M. E. for the TAXUS II Study Group. *Circ. Clin. Invest. Rep.* **2003**, *108*, 788.
- (21) Silber, S. *J. Interv. Cardiol.* **2003**, *16*, 485.
- (22) Seal, B. L.; Otero, T. C.; Panitch, A. *Mater. Sci. Eng., R* **2001**, *34*, 147.
- (23) McCaig, C. D.; Rajnicek, A. M.; Song, B.; Zhao, M. *Physiological Reviews* **2005**, *85*, 943.
- (24) Iijima, S. *Nature* **1991**, *354*, 56.
- (25) Bianco, A.; Kostarelos, K.; Partidos, C. D.; Prato, M. *Chem. Commun.* **2005**, 571.
- (26) Lin, Y.; Taylor, S.; Li, H.; Fernando, K. A. S.; Qu, L.; Wang, W.; Gu, L.; Zhou, B.; Sun, Y.-P. *J. Mater. Chem.* **2004**, *14* (4), 527.
- (27) Correa-Duarte, M. A.; Wagner, N.; Rojas-Chapana, J.; Morszeck, C.; Thie, M.; Giersig, M. *Nano Lett.* **2004**, *4* (11), 2233.
- (28) Mattson, M. P.; Haddon, R. C.; Rao, A. M. *J. Mol. Neurosci.* **2000**, *14*, 175.
- (29) Gheith, M. K.; Sinani, V. A.; Wicksted, J. P.; Matts, R. L.; Kotov, N. A. *Adv. Mater.* **2005**, *17*, 2663.
- (30) Cherukuri, P.; Bachilo, S.; Litovsky, S. H.; Weisman, R. B. *J. Am. Chem. Soc.* **2004**, *126*, 15638.
- (31) Zanello, L. P.; Zhao, B.; Hu, H.; Haddon, R. C. *Nano Lett.* **2006**, *6* (3), 562.
- (32) Huang, Z. M.; Zhang, Y. Z.; Kotaki, M.; Ramakrishna, S. *Compos. Sci. Technol.* **2003**, *63*, 2223.

Table 1. Properties of SIBS/SWNT Dispersions

solution or dispersion	conductivity ( $\mu\text{S}/\text{cm}$ ) <sup>a</sup>	surface tension (mN/m) <sup>b</sup>	viscosity (mPa S) <sup>c</sup>
13 wt % SIBS	0	34.46	2855.71
5 wt % SIBS/0.3% SWNT	77.1	31.11	99.15
9 wt % SIBS/0.3% SWNT	86.1	24.00	193.58
13 wt % SIBS/0.3 %SWNT	94.7	23.32	385.58

<sup>a</sup> Determined by a model 20 pH/conductivity meter (Denver Instruments). <sup>b</sup> Determined by a KSV contact angle analyzer (goniometer, KSV Instruments Ltd). <sup>c</sup> Determined by a DV-II viscometer (Brookfield Engineering Lab., Inc.), shear rate using  $20\text{ s}^{-1}$  for viscosity testing.

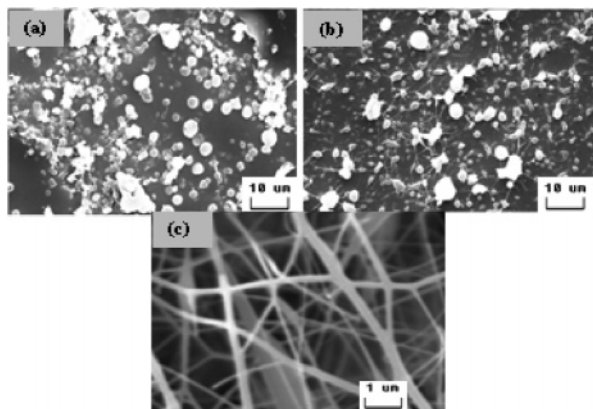


**Figure 1.** SEM images of electrospun fibers obtained from toluene dispersions containing (a) 5% (w/v) SIBS/0.3% (w/v) SWNT, (b) 9% (w/v) SIBS/0.3% (w/v) SWNT, and (c) 13% (w/v) SIBS/0.3% (w/v) SWNT. The increasing ratio of interconnecting fiber to bead structure with increasing SWNT concentration is shown. The presence of SIBS at 12% or greater gave a well-interconnected porous structure.

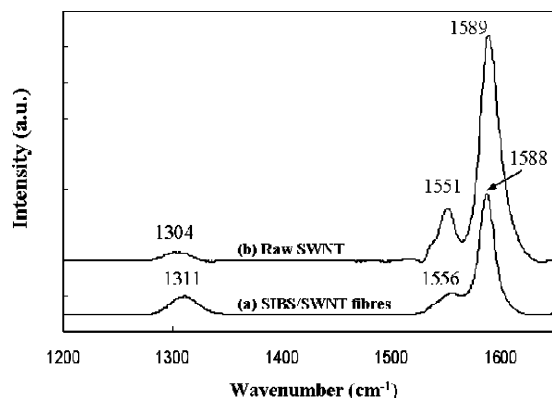


**Figure 2.** Raman spectra of (a) 13% (w/v) SIBS/0.3% (w/v) SWNT blend fibers and (b) raw SWNT (using 632.8 nm diode laser excitation on 300 lines/mm grating at room temperature).

here (Table 1). Pure SIBS is highly resistant. However, the conductivity of dispersions improved significantly with addition of SWNT. The surface tension of dispersions decreased and the viscosity increased with increasing concentration of SIBS.

Fibers could not be electrospun from nonconductive SIBS alone. However, with the addition of SWNT, nonwoven mats were collected on the gold-coated mylar collector. SEM images showed that few fibers were obtained when the concentration of SIBS was less than 7% (w/v) in the dispersion (Figure 1a), perhaps because of the low viscosity of these solutions. The fibrous structure of the mats improved significantly when the concentration of SIBS was increased from 7 to 11% (w/v) (Figure 1b); and at concentrations above 12% (w/v) SIBS, nonwoven mats of composite fibers could be obtained with well-interconnected structure (Figure 1c). The composite fibers ranged from 30 to 350 nm in diameter.

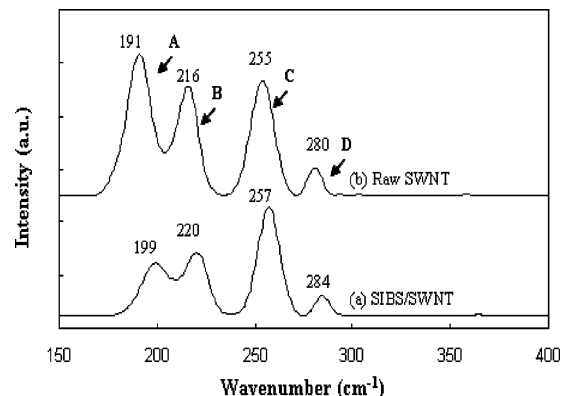


**Figure 3.** Radial breathing mode Raman spectra of (a) 13% (w/v) SIBS/0.3% (w/v) SWNT blend fibers and (b) raw SWNT (using 632.8 nm diode laser excitation on 300 lines/mm grating at room temperature).

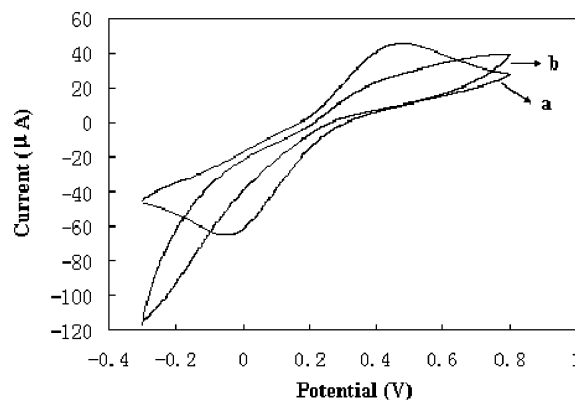


**Figure 4.** Cyclic voltammograms in 1 mM  $\text{K}_3\text{Fe}(\text{CN})_6$ /phosphate buffer solution of (a) electrospun fibers from 13% (w/v) SIBS/0.3% (w/v) SWNT on ITO glass, and (b) bare ITO glass slide. Scan rate: 50 mV/s.

SEMs showed the high surface area and microporous structure of the electrospun fibers (Figure 1c).

The presence and distribution of SWNTs in the composite fibers were confirmed using Raman spectroscopy (JYHR800) with 632.8 nm diode laser excitation on 300 lines/mm grating at room temperature. Figures 2 and 3 show G-band and radial breathing mode (RBM) Raman spectra of 0.3% (w/v) SWNT/13% (w/v) SIBS electrospun fibers in comparison with that of raw SWNTs. According to Rao et al.,<sup>33</sup> peaks in the 100–275  $\text{cm}^{-1}$  range (RBM) and in the 1500–1600  $\text{cm}^{-1}$  range (tangential (stretching) modes) should be prominent in Raman spectra of SWNT. Figure 2a shows three classical peaks that could be attributed to SWNT: 1588  $\text{cm}^{-1}$  (from the graphitic sheets), 1556  $\text{cm}^{-1}$  (stretching mode of SWNT), and 1311  $\text{cm}^{-1}$  (defects in SWNT).<sup>34</sup> The observed shifts in RBM (Figure 3) indicate interactions between SIBS and SWNT. Raman spectra were consistent across the electrospun

(33) Rao, A.; Chen, J.; Richter, E. *Phys. Rev. Lett.* **2001**, *86*, 3895.

(34) Basca, W. S.; Ugarte, D.; Chatelain, A. *Phys. Rev. B* **1994**, *50*, 15473.

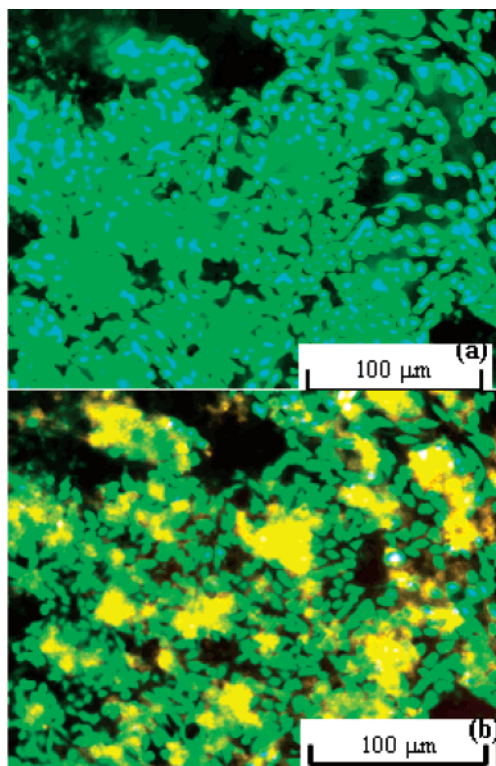


**Figure 5.** Fluorescence microscope images of L-929 cells growing on SWNT/SIBS electrospun fibers. Figure 5a shows calcein-stained cells using fluorescence detection only. Figure 5b shows the same field with the addition of transmission (white light) imaging to show the position of SWNT/SIBS fibers (dark regions).

mats, indicating that SWNTs were well dispersed through the composite fibers.

Cyclic voltammograms were obtained using the electrospun SIBS/SWNT mats on ITO glass. Figure 4 shows a CV of 13% (w/v) SIBS/0.3% (w/v) SWNT electrospun fibers on ITO glass compared with that of bare substrate. This indicates that electrospun fibers have a much higher charge capacity and higher surface area than the bare ITO glass. A redox couple observed at 0.48 and  $-0.05$  V (vs Ag/AgCl)

indicates an electroactivity for the composite fibers that is attributed to the presence of SWNTs.

L-929 is a mouse fibroblast line that is commonly used to assess the cytotoxicity of potential substrates for cell growth. Calcein AM is a vital dye that diffuses across the plasma membrane and is cleaved by intracellular esterases to yield the membrane impermeant, fluorescent calcein product. Calcein AM therefore may be used as a cell viability dye, staining metabolically active cells bright green. L-929 cells were seen to adhere to and grown on 0.3% (w/v) SWNT/13% (w/v) SIBS electrospun fibers, such that clusters of viable cells could be visualized by 72 h of culture time (Figure 5a). The cells grew as well on SWNT/SIBS electrospun fibers as on a gold-mylar substrate, as shown using a combination of transmission and fluorescence microscopy (Figure 5b), the rate of growth on the electrospun fibers being similar to that on polystyrene tissue culture plastic (not shown). These results suggest that SWNT/SIBS electrospun fibers are biocompatible substrates.

In summary, we have shown that nanofibres of SIBS/SWNT can be obtained from SIBS/SWNT toluene dispersions by electrospinning. The resulting fibers have a high surface area and well-interconnected microporous structure, indicating potential applications in areas requiring good mass transport. The presence of SWNTs through the electrospun fibers rendered the composite fibers conductive and electroactive. This useful combination of properties, combined with the compatibility of the SIBS/SWNT fibers with L-929 cells, opens up the possibility of using these conductive materials as substrates for studies of the effects of electrical stimulation on cell growth and suggests possible applications in biomedical fields such as in tissue engineering.

**Acknowledgment.** This work was funded in part by the Australian Research Council. SIBS was supplied by Boston Scientific, USA.

CM070002J